

Research Article

Emil Smyk*, Sylwester Wawrzyniak, and Kazimierz Peszyński

Synthetic jet actuator with two opposite diaphragms

<https://doi.org/10.2478/mme-2020-0004>

Received Oct 21, 2019; accepted Mar 04, 2020

Abstract: The synthetic jet actuators are one of the most investigated types of actuators used in heat transfer and active flow control. The energetic efficiency of actuators is a key parameter determining the possibility of device use. The actuators with two or more diaphragms have higher efficiency than the actuators with only one. The paper presents the investigations of the acoustic synthetic jet actuator with two opposite diaphragms. In the paper, synthetic jet velocity, Reynolds number and the energetic efficiency as a function of oscillating actuator frequency, for a different cavity, orifice configuration and one real input power $P_0 = 2 \text{ W}$ were studied. The possibility of theoretical calculation of first and second resonance frequency were checked. The coupling ratio for actuators was calculated. The maximum energetic efficiency was $\eta = 8.67\%$ and Reynolds number $Re = 8503$. The possibility of using the same dependencies and rules during the design of actuators with two opposite diaphragms as in the case of actuators with one diaphragm was demonstrated. The results may be useful in the design of the actuators of the two membranes.

Keywords: Zero-net-mass flux, coupling ratio, two diaphragms actuator, efficiency

1 Introduction

Synthetic jet (SJ) is formed by periodic expulsion and ingestion of fluid at the exit of a nozzle so the average over

time mass flow rate through the orifice is zero during one full operation cycle. SJ is also called as zero-net mass-flux (ZNMF). A typical synthetic jet actuator (SJA) is a resonant cavity with an orifice or a nozzle and one of its walls is replaced by a movable element: loudspeaker diaphragm, piezoelectric, piston or others. During the expulsion phase, the fluid steam moves away from the nozzle and edge vortices are generated on its edge. The environmental fluid fills the SJA cavity during the ingestion phase. Thanks to formation of the edge vortices, the SJs are used in many fields of technology including: aviation [1, 2], transport [3, 4], heat transport [5–7], active flow control [7–9] and so on. Due to many applications, SJs are produced with the use of many types of different actuators (in terms of construction and type) so as to increase the SJ efficiency or velocity.

Kordík and Trávníček [10, 11] studied the dependence between the integral quantities (volumetric flux, momentum flux and kinetic energy flux) of SJs and the nozzle geometry. They demonstrated that the use of a nozzle with rounded edges increases the SJ characteristic velocity even by 18.5%, as compared to the same SJA with a sharp-edged nozzle [10]. The results were even higher (43.3% for momentum flux and 70.8% for kinetic energy flux) for other measured parameters. Kordík and Trávníček [11] investigated the optimal volume of the nozzle optimal diameter. This issue is extended in [12]. Basing on experimental and theoretical studies, the authors indicate the ratios between diameters of the nozzle and the diaphragm for which efficiency of the SJA was the largest. The tests were performed with the use of two loudspeakers, nine nozzle diameters and ten supplied power levels. The highest achieved efficiency was 15% and 11% for the tested loudspeakers [12].

Gil and Strzelczyk [13] presented the tests of seven different SJAs and three supply voltage levels. The paper presented the dependence of SJ velocity, Reynolds number and efficiency on the supply frequency. Additionally, the dependence of SJ parameters on the actuator geometrical size (nozzle diameter, nozzle thickness and depth of cavity) was presented. During the tests, the constant supply voltage value was used.

***Corresponding Author: Emil Smyk:** Department of Mechanical Engineering, UTP University of Science and Technology, Al. Prof. S. Kaliskiego 7, Bydgoszcz, 85-796, Poland; Email: emil.smyk@utp.edu.pl

Sylwester Wawrzyniak: Department of Mechanical Engineering, UTP University of Science and Technology, Al. Prof. S. Kaliskiego 7, Bydgoszcz, 85-796, Poland; Email: sylas@utp.edu.pl

Kazimierz Peszyński: Department of Mechanical Engineering, UTP University of Science and Technology, Al. Prof. S. Kaliskiego 7, Bydgoszcz, 85-796, Poland; Email: peszyn@utp.edu.pl

The second method used for an increase in SJ parameters, other than changing the actuator geometrical size, was its construction changing. In studies of Greco *et al.*, [14, 15] a twin and single SJ were compared. A twin SJA was understood as an actuator with two cavities separated by a diaphragm. This type of actuator generates two ‘single’ SJs using nozzles placed mostly close to each other. Among others, a twin SJ may be used in cooling systems due to a higher turbulence level.

The other type of SJ is a hybrid synthetic jet (HSJ). The HSJ actuator has the same layout structure as a classic SJA, but it is additionally equipped with a fluidic diode, a specially shaped channel that has a significantly higher hydraulic resistance in one direction than in the other. The diode works similarly to other nozzles. Kordík *et al.* [16] compared the SJ and HSJ generated by similar actuators according to the same input real power. It has been proved that the use of HSJ can increase velocity by nearly 15–23% and the energy efficiency by nearly 41–48%. The resonance frequency of actuators was different – 87 Hz for SJA and 100 Hz for HSJ actuator.

Among others, the method for improving or changing the SJ parameters can be improved by modification of the actuator cavity shape [17], use of two or more actuators operating together with the nozzle, placed next to each other [18, 19], the use of double orifice [6, 20] or use of more than one diaphragm [21–23]. The benefits of using two diaphragms, instead of one, are described in [24, 25]. Two diaphragms are also used for the HSJ [16, 26].

Smyk [25] compared three SJAs with one and two diaphragms with the same input real power, frequency and similar actuator arrangement. The first actuator with one diaphragm operates in normal conditions, a small closed cavity is placed behind the diaphragm of the second actuator with one diaphragm. The actuator with two diaphragms is a combination of the two previous ones – one diaphragm with and one without a small closed cavity behind it. The use of two diaphragms increases the velocity by 28.2% and electrical efficiency by 48.5% in relation to the actuator with one diaphragm, which operates in normal conditions.

In the paper, the synthetic jet actuators with two opposite diaphragms will be investigated for different cavity height and nozzle diameter. The results will be compared with the theoretical features used in the design of classic actuator, as resonant frequencies and coupling ratio.

2 Parameters

SJs generated using the fluid periodic pulsation are most often characterized by non-dimensional parameters, Reynolds number, Re , and stroke length, L^* . The velocity characteristic for Reynolds number and the stroke ratio can be defined as:

$$U_0 = \frac{1}{TS_n} \int_0^{T_E} \int_{S_n} u(t) dS dt \quad (1)$$

where S_n is the nozzle exit cross-section area, dS is the differential element of S_n , $u(t)$ is the velocity measured along the nozzle axis, T_E is the time of fluid extrusion from the actuator, $T = 1/f$ is the actuation period, f is the actuation frequency. Parameters Re and L^* are evaluated according to the following definition [16, 27, 28]:

$$Re = \frac{U_0 D_n}{\nu}, \quad L^* = \frac{L_0}{D_n} = \frac{U_0}{f D_n} \quad (2)$$

where D_n is the nozzle diameter, ν is the kinematic viscosity of the working fluid ($\nu = 1.82 \cdot 10^{-5} \text{ m}^2 \cdot \text{s}^{-1}$, air). Among others, non-dimensional parameters used for the SJ description should be mentioned: Strouhal number St and Stokes number S , defined as follows [26, 29]:

$$St = \frac{\pi}{L^*}, \quad S = \left(2\pi \frac{Re}{L^*} \right)^{0,5} \quad (3)$$

One of the most important parameters used for the SJAs tests is energetic efficiency η . In the used model, energy efficiency can be understood as a ratio of the time-average kinetic energy flux E_0 , calculated from the extrusion stroke with input real power P_{RMS} . For the slug and a sinusoidal model $u(t)$, the energy efficiency can be calculated from [26, 30]:

$$\eta = \frac{E_0}{P_0} = \frac{\frac{\pi}{3} \rho S_n U_0^3}{\frac{1}{T} \int_0^T i(t) e(t) dt} \quad (4)$$

where ρ is the density of the working fluid ($\rho = 1.18 \text{ kg} \cdot \text{m}^{-3}$), $i(t)$ is waveforms of the input electric current and $e(t)$ is waveforms of the input electric voltage.

Additionally, the stroke length will be used as a formation criterion of SJ. The paper [31, 32] demonstrated that the formation criterion of the synthetic jet can be featured as:

$$L^* > 0.5 \quad (5)$$

If this condition is not fulfilled, then SJ will be not generated.

3 Experiment arrangement and method

The actuator designed for the purpose of the tests is shown in Figure 1. The actuator consists of two universal speakers Monacor SP-6/4SQS with magnetic shielding (impedance $Z = 4 \Omega$, power rating $P = 3 \text{ W}$, frequency range $f = 3 \div 16000 \text{ Hz}$) – placed opposite each other; actuator body printed using 3D technologies from polylactide (PLA) – the print errors were additionally corrected. The loudspeakers were fastened using four bolts and the speaker foam sealing tape was bonded between speakers and the body – not shown in Figure 1. Tests were carried out for three nozzle diameters $D_n = 5, 10, 20 \text{ mm}$, three cavity heights $h = 15, 25, 45 \text{ mm}$ and one nozzle length $L_n = 5 \text{ mm}$. During tests, a sharp edge nozzle was used. Additionally, in Figure 1, the used coordinate system is presented – x is the axial and r is radial coordinate.

The actuator was supplied with the harmonic electrical current that was generated by a Rigol DG4162 waveform generator and provided in SeoUm Pa-940/2 amplifier. The actuator input real power was constant, $P_0 = 2 \text{ W}$ with maximal error 3%. The actuators were tested for frequency range $f = 10 \div 1000 \text{ Hz}$ with frequency step value 10Hz. Velocity $u(t)$ was measured in the nozzle axis at an approxi-

mate distance 0.5 mm from the nozzle exit area. MiniCTA 55T30 Dantec Dynamics hot-wire anemometer with a single wire probe 55P16 and NI9215 data acquisition device was used for velocity measurements. The anemometer was calibrated within range $0.5 \div 25 \text{ m}\cdot\text{s}^{-1}$. The velocity error was less than 5% for velocity larger than $1 \text{ m}\cdot\text{s}^{-1}$ and was 15% for velocity lower than $1 \text{ m}\cdot\text{s}^{-1}$. The number of samples was constant during all measurements, $n = 512$, and the sampling frequency was evaluated as $f_s = n \cdot f / 6$. This standard is more demanding than Nyquist frequency and velocity U_0 is always calculated on the basis of 6 operation periods of the actuator.

4 Results

Figure 2 presents the selected parameters of SJ and SJA as the function of the actuator operation frequency f . The compared SJA had the same nozzle diameter, $D_n = 10 \text{ mm}$, and different cavity height h – case 1. Parameters of this and other actuators are presented in Table 1. The dependence between velocity U_0 and frequency f is shown in Figure 2a. The resonant frequencies can be determined as the local maximum of velocity. The natural frequency f_n , as the first maximum and the Helmholtz frequencies f_H , as the second maximum. The natural frequency can be determined for each variant in case 1 and is $f_n = 240 \text{ Hz}$ at the cavity height $h = 15$ and 25 mm , and is $f_n = 260 \text{ Hz}$ at the cavity height $h = 45 \text{ mm}$. The Helmholtz frequencies are $f_H = 760 \text{ Hz}$ at the cavity height $h = 25 \text{ mm}$ and $f_H = 520 \text{ Hz}$ at the cavity height $h = 45 \text{ mm}$. At cavity height $h = 15 \text{ mm}$, the Helmholtz frequency is higher than the frequency range.

In the first case, the maximum velocity was registered at natural frequencies. However, the smaller the difference between the velocity at a natural frequency and Helmholtz frequencies, the higher is the cavity. SJ velocity is $U_0 = 12.15 \text{ m}\cdot\text{s}^{-1}$ at the cavity height $h = 15 \text{ mm}$, $U_0 = 10.53 \text{ m}\cdot\text{s}^{-1}$ at

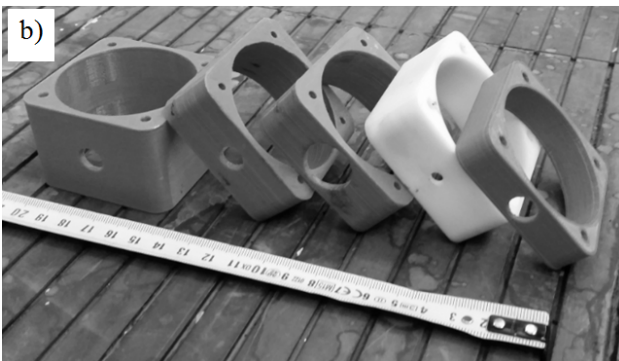
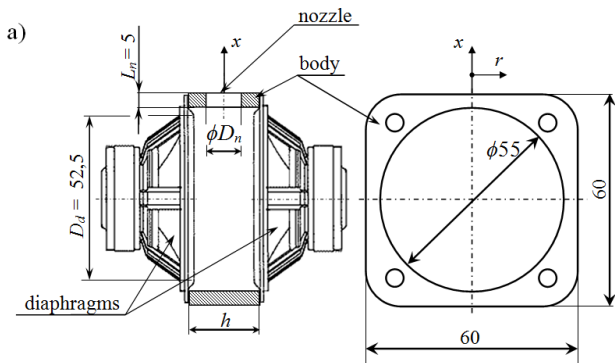


Figure 1: (a) Schematic view of the investigated synthetic jet actuator, (b) Photo of the actuators bodies

Table 1: Actuator parameters and investigation conditions

	D_n mm	h mm	L_n mm	h/D_n -	P_0 W	f Hz	
Case 1	10	15	5	1.5	2	10–1000	
		25		2.5			
		45		4.5			
Case 2	10	25	5	5	2	10–1000	
				10			2.5
				20			1.25

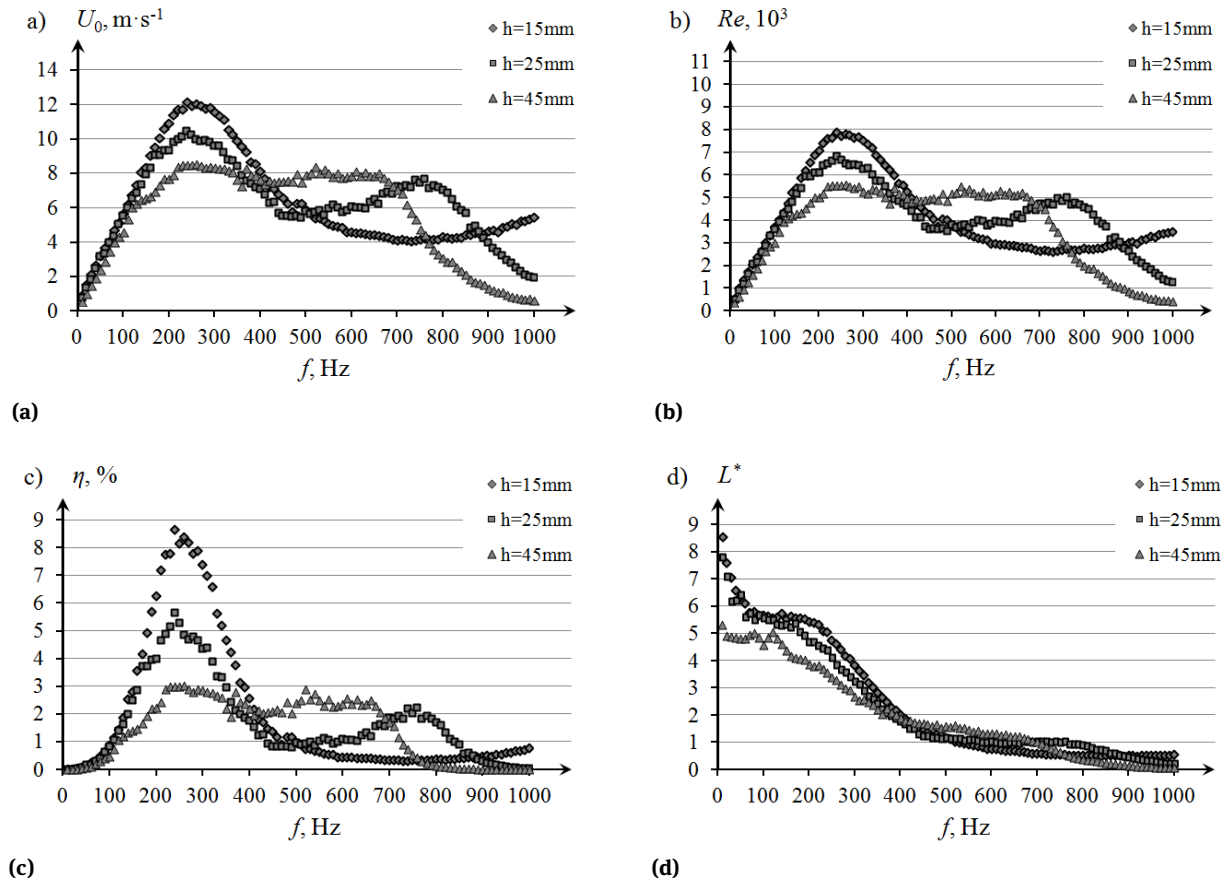


Figure 2: Velocity U_0 (a), Reynolds number Re (b), efficiencies η (c) and stroke length L^* (d) of SJ as the function of the actuator operation frequency f – by different cavity height h (Case 1: $h = 10, 25$ and 45 mm, $D_n = 10$ mm, $P_0 = 2$ W).

the cavity height $h = 25$ mm, $U_0 = 8.53 \text{ m}\cdot\text{s}^{-1}$ at the cavity height $h = 45$ mm.

Figure 2b presents the Reynolds number as a function of the actuator frequency. Reynolds number graph is similar to the velocity graph – constant nozzle diameter $D_n = 10$ mm and constant conditions of investigations ($\nu = \text{const}$). Reynolds number is $Re = 7910$ at the smallest cavity height $h = 15$ mm, $Re = 6856$ at the medium cavity height $h = 25$ mm and $Re = 5558$ at the biggest cavity height $h = 45$ mm – all results at natural frequencies.

Figure 2c presents the electrical efficiency of the SJA as a function of the actuator frequency. The obtained efficiency is quite good and is even $\eta = 8.67\%$ at the smallest cavity height $h = 15$ mm. The efficiency at the cavity height $h = 45$ mm is almost equal for natural and Helmholtz frequencies – $\eta = 2.91\%$ and $\eta = 2.90\%$, respectively. For other heights, this difference is more significant.

Figure 2d presents the SJ stroke length as a function of the actuator frequency. The formation criterion of SJ is fulfilled when the frequency is $f < 890$ Hz for cavity height $h =$

25 mm, and $f < 780$ Hz for cavity height $h = 45$ mm. For cavity height $h = 15$ mm, the stroke length is always larger than 0.5; however, at frequency $f > 800$ Hz, the stroke length value is close to the limit value.

Figure 3 presents the selected parameters of SJ and SJA as a function of the actuator operation frequency f . The compared SJA had the same cavity heights $h = 25$ mm and a different nozzle diameter D_n – case 2 (Table 2). The velocity of SJ as a function of the actuator frequency is presented in Figure 3a. On the basis of velocity distribution, the characteristic frequencies of the actuator can be determined. The SJ velocity assumes the highest value of the first resonant frequency (natural frequency) for nozzle diameter $D_n = 10$ and 20 mm and the second frequency (Helmholtz frequency) for nozzle diameter $D_n = 5$ mm. The Helmholtz frequency cannot be designed for nozzle diameter $D_n = 20$ mm because it is outside the frequency measurement range. Natural frequency is $f_n = 240$ Hz for nozzle diameter $D_n = 5, 10$ mm and $f_n = 270$ Hz for nozzle diameter $D_n = 20$ mm. Helmholtz frequency is $f_H = 520$ Hz for nozzle di-

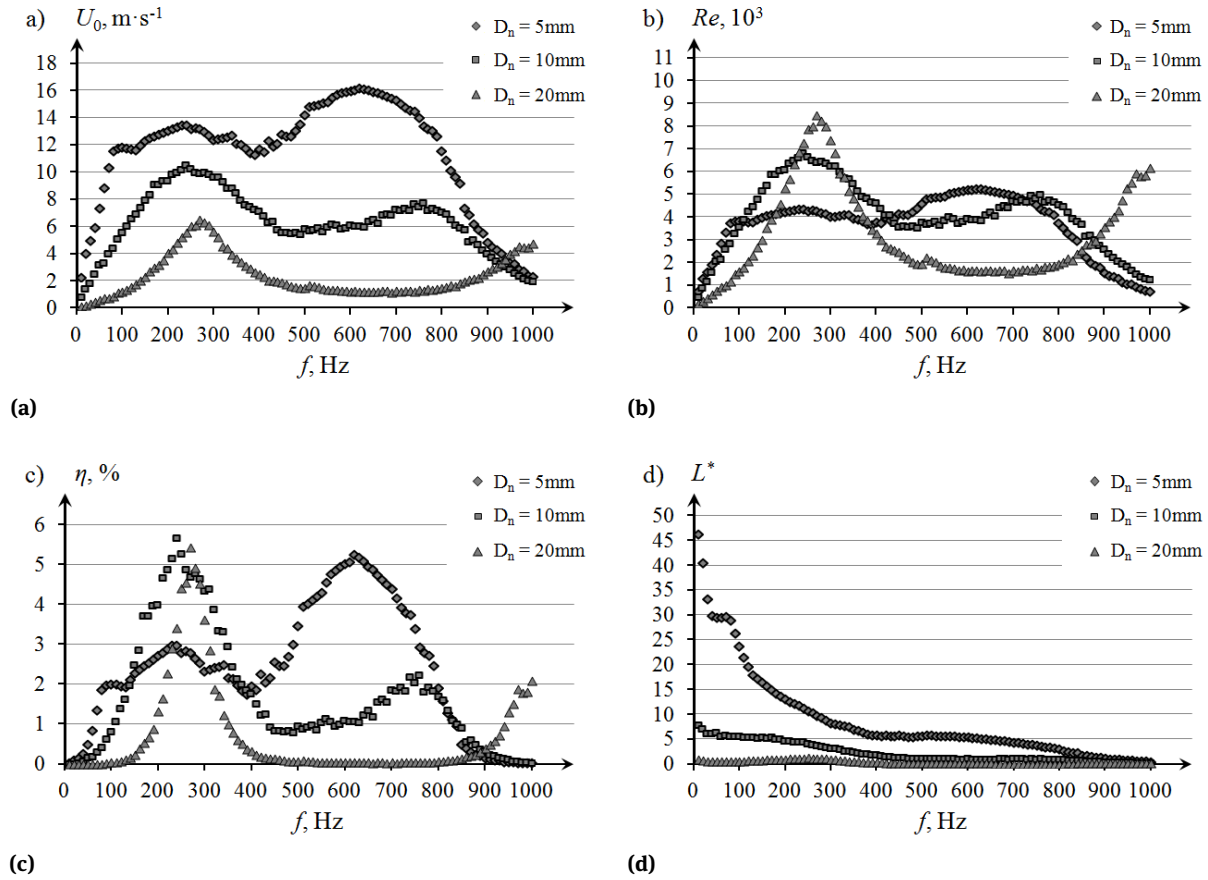


Figure 3: Velocity U_0 (a), Reynolds number Re (b), efficiencies η (c) and stroke length L^* (d) of SJ as function of the actuator operation frequency f – by different nozzle diameter D_n (Case 1: $h = 25$ mm, $D_n = 5, 10$ and 20 mm, $P_0 = 2$ W)

iameter $D_n = 5$ mm and $f_H = 760$ Hz for nozzle diameter $D_n = 10$ mm. The maximal value of SJ velocity is $U_0 = 16.26 \text{ m}\cdot\text{s}^{-1}$ for nozzle diameter $D_n = 5$ mm and Helmholtz frequency $f_H = 620$ Hz, $U_0 = 10.53 \text{ m}\cdot\text{s}^{-1}$ for nozzle diameter $D_n = 10$ mm and natural frequency $f_n = 240$ Hz, $U_0 = 6.53 \text{ m}\cdot\text{s}^{-1}$ for nozzle diameter $D_n = 20$ mm and natural frequency $f_n = 240$ Hz.

Figure 3b shows the dependence between Reynolds number and the actuator operating frequency. The maximal value of SJ Reynolds number is $Re = 8503$ for the biggest value of nozzle diameter $D_n = 20$ mm. The nozzle diameter is very important because the biggest Reynolds number corresponds to a smaller value of SJ velocity – considering only natural frequency for nozzle diameter $D_n = 10, 20$ mm and Helmholtz frequency for nozzle diameter $D_n = 5$ mm. Reynolds number is $Re = 6856$ for the medium value of nozzle diameter $D_n = 10$ mm and $Re = 5293$ for the biggest value of nozzle diameter $D_n = 5$ mm.

The electrical efficiencies of SJA are shown in Figure 3c. The maximal efficiencies are very similar for the

compared actuators if the previously mentioned frequencies are taken into account. The SJA electrical efficiency is $\eta = 5.26\%$ for nozzle diameter $D_n = 5$ mm, $\eta = 5.67\%$ for nozzle diameter $D_n = 10$ mm and $\eta = 5.42\%$ for nozzle diameter $D_n = 20$ mm.

Figure 3d presents the stroke length as a function of frequency. The stroke length fulfills Eq. (2.5) for all cases discussed in detail. However, the stroke length is smaller than 0.5 for frequency $f > 350$ Hz and nozzle diameter $D_n = 20$ mm, while it is $f > 880$ Hz for nozzle diameter $D_n = 5$ mm and $f > 980$ Hz for nozzle diameter $D_n = 10$ mm.

5 Discussion

SJA has two characteristic frequencies. First, natural frequency, f_n , is the resonance frequency of the diaphragm or piston used in SJA. Second, Helmholtz frequency f_H , is the resonance frequency of some volume of fluid in the actuator nozzle. The values of both frequencies are related to

each other but there exist many ways to calculate them. In the studies by Girfoglio *et al.*, [33] natural frequency was defined as:

$$f_n = \frac{1}{2\pi} \sqrt{\frac{K_d}{m_d}} \quad (6)$$

where K_d is the actuator diaphragm spring constant and m_d is the diaphragm total mass. It is a basic dependence and it does not include the influence of the fluid in the nozzle during the diaphragm operation. Kordík and Trávníček [12] feature natural frequency as:

$$f_n = \frac{1}{2\pi} \sqrt{\frac{K_d}{m_d + \left(\frac{D_d}{D_n}\right)^4 m_n}} \quad (7)$$

where m_n is the fluid mass in the actuator nozzle, calculated as $m_n = \rho L_e S_n$ and $L_e = L_n + 8 \cdot D_n / (3\pi)$. Eq. (5.2) takes into account the influence of nozzle shape on the diaphragm operation. Broučková and Trávníček^[26] offer another method for natural frequency calculation:

$$f_n = \frac{1}{2\pi} \left(\frac{D_n}{D_d}\right) \sqrt{\frac{K_p}{2\rho L_e}} \quad (8)$$

where K_p is the diaphragm spring constant defined by the ratio of overpressure p , which caused a steady displacement of diaphragm Δx , $K_p = p/\Delta x$.

The values of experimental and theoretical (Eq. (6), (7) and (8)) natural frequencies f_n are presented in Table 2 ($\rho = 1.18 \text{ kg}\cdot\text{m}^{-3}$, $K_d = 3050 \text{ N}\cdot\text{m}^{-1}$, $K_p = 1.3\cdot 10^6 \text{ N}\cdot\text{m}^{-3}$, $m_d = 2.763\cdot 10^{-3} \text{ kg}$ – determined in an auxiliary experiment).

Absolute errors of theoretical data – respect to the experimental data – for values calculated from Eq. (6) and (7) are similar for all actuators. It is about 30% for Eq. (6) and about 40% for Eq. (7). The errors in the case of Eq. (8) are the smallest but strongly dependent on ratio D_n/D_d . In case of actuator of $D_n = 5 \text{ mm}$ and $h = 25 \text{ mm}$, the absolute error is nearly 61%; in other cases it is 27%. The natural frequency experimental value and the natural frequency theoretical value calculated from Eq. (8), presented in [26], are the same ($D_n/D_d = 0.15$). In the present case, the theoretical value would be 240 Hz only if the ratio $D_n/D_d = 0.37$ ($D_n = 19.42 \text{ mm}$).

All theoretical equations were calculated with LEM method. The difference between them is the result of different simplifications of the physical model. All models included only one diaphragm, eventually, two diaphragms operated in the same phase. Theoretically, it is enough but in the real actuator with two diaphragms, they can operate with a small delay relative to each other and the used loudspeakers may have different properties. The paper [24] demonstrated the impact of phase shift between two diaphragms on the SJs parameters, but the impact of phase

shift on resonant frequencies probably isn't yet investigated. It is similar for diaphragms operated in the same phase but with other conditions, see [25].

The second frequency is the frequency of some part of fluid oscillated in the actuator nozzle. Helmholtz frequency is featured as [34]:

$$f_H = \frac{1}{2\pi} \sqrt{\frac{\gamma \cdot S_n^2 \cdot p}{V_c \cdot m_n}} \quad (9)$$

where γ is the air specific heat ratio, p is the ambient pressure, V_c is the actuator cavity volume. Theoretical and experimental Helmholtz frequencies are presented in Table 2.

In case of actuator at $D_n = 10 \text{ mm}$, $h = 15 \text{ mm}$ and at $D_n = 20 \text{ mm}$, $h = 25 \text{ mm}$ the experimental value of Helmholtz frequency is larger than 1000 Hz and is not experimentally determined. However, for the actuator operation frequency larger than 1000 Hz, the formation criterion of SJ [31] is not met (Figure 2d and 3d).

de Luca *et al.* [34] presents a model of a piezoelectric actuator operation, but some parameters can also be used for acoustic actuators [13]. Especially, coupling ratio CR of the two oscillator systems:

$$CR = \left(\frac{\omega_{ps}}{\omega_n}\right)^2 \quad (10)$$

where ω_{ps} is the frequency of pneumatic spring of the actuator cavity:

$$\omega_{ps} = \sqrt{\frac{\gamma \cdot S_c^2 \cdot p}{V_c \cdot m_d}} \quad (11)$$

and

$$\omega_n = 2\pi f_n \quad (12)$$

CR represents the ratio of air stiffness (air in the cavity of volume V_c and cross-section area S_c) to membrane stiffness. If $CR \ll 1$, the membrane dynamics is uncoupled from the acoustic oscillator. For such an oscillation, the natural frequency is higher than the Helmholtz frequency. In other words, the bigger is the coupling ratio CR , bigger is the difference between the value of natural and Helmholtz frequencies. This relationship is clearly visible in Figure 2a and 3a.

In Case 1, for cavity height $h = 25 \text{ mm}$, the coupling ratio $CR = 0.85$ and the distance between experimental normal and Helmholtz frequency is 520 Hz, and for cavity height $h = 45 \text{ mm}$, the coupling ratio $CR = 0.37$, this distance is 250 Hz (see Table 2).

de Luca *et al.* [34] observe that the difference between the two frequencies depends on the cavity height. For $f_n \ll f_H$, the difference between the two eigenvalues $(f_n^2 - f_H^2)/f_H^2$ does not depend on the distance h/D_n (Figure 4a, directional coefficient close to zero), and therefore,

Table 2: Experimental and theoretical values of natural and Helmholtz frequency

	D_n	h	exp. f_n	f_n , Eq. (6)	f_n , Eq. (7)	f_n , Eq. (8)	exp. f_H	f_H , Eq. (9)	CR
	mm	mm	Hz	Hz	Hz	Hz	Hz	Hz	-
Case 1	10	15	240	167	144	174	-	882	1.41
		25	240	167	144	174	760	683	0.85
		45	270	167	144	174	520	509	0.37
Case 2	10	5	240	167	122	94	620	431	0.85
		25	240	167	144	174	760	683	0.85
		20	270	167	155	305	-	1034	0.67

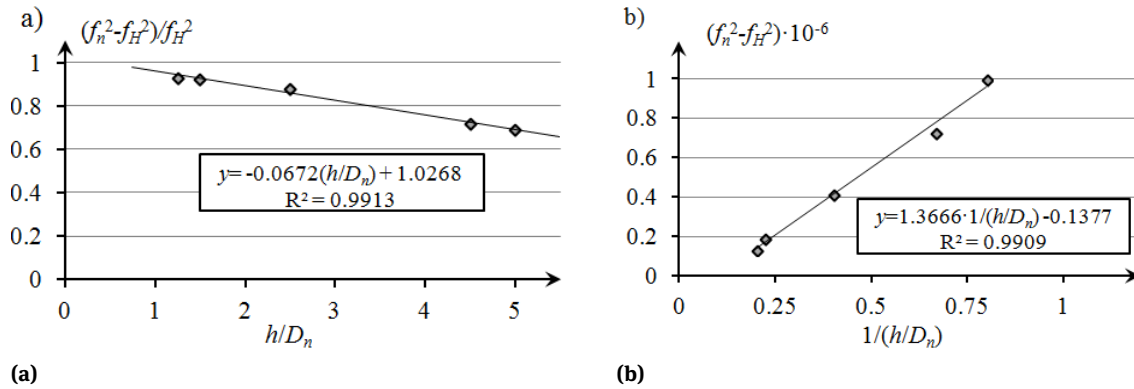


Figure 4: The impact of the difference between the two eigenvalues of natural and Helmholtz frequencies on the cavity height, (a) $(f_n^2 - f_H^2)/f_H^2$ as a function of h/D_n (b) $(f_n^2 - f_H^2)$ as a function of $1/(h/D_n)$

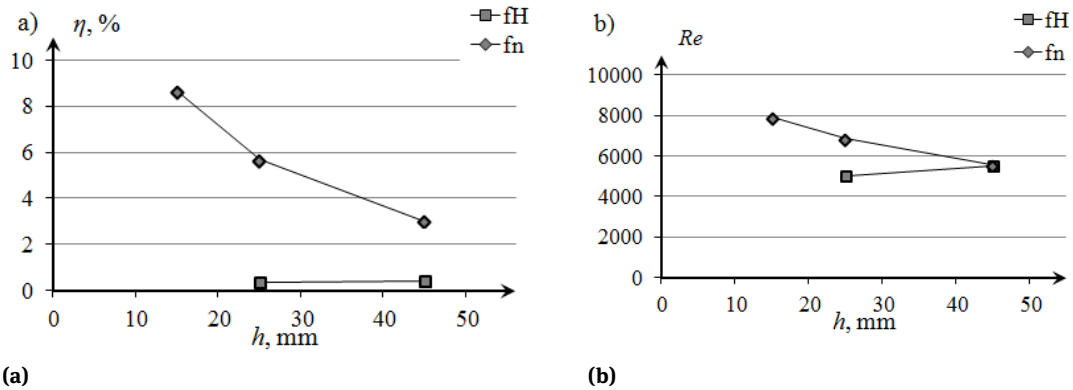


Figure 5: (a) actuator efficiency η and (b) Reynolds number Re as a function of cavity height for natural f_n and Helmholtz f_H resonance frequencies

$(f_n^2 - f_H^2)$ depends on $1/(h/D_n)$ (Figure 4b). It means that the peak between two frequencies increases with the cavity decreasing (Figure 3a) and the diameter increasing (Figure 4a), like it was observed. It can be assumed that if $f_n \ll f_H$, then $(f_n^2 - f_H^2)/f_H^2$ depends on distance h/D_n [34].

Figure 5 shows the dependence of actuator efficiency η and Reynolds number Re on the actuator cavity height for natural f_n and Helmholtz f_H frequencies. Larger the effi-

ciency and Reynolds number, the smaller the cavity height is in the case of natural frequency; in the case of Helmholtz frequency, the dependence is opposite, but the parameters changes are negligible – the Helmholtz frequency is the resonant frequency of some volume of fluid in the nozzle and the volume of cavity influence on the value of frequency but only slightly on fluid parameters (by so small pressure, the air is almost incompressible).

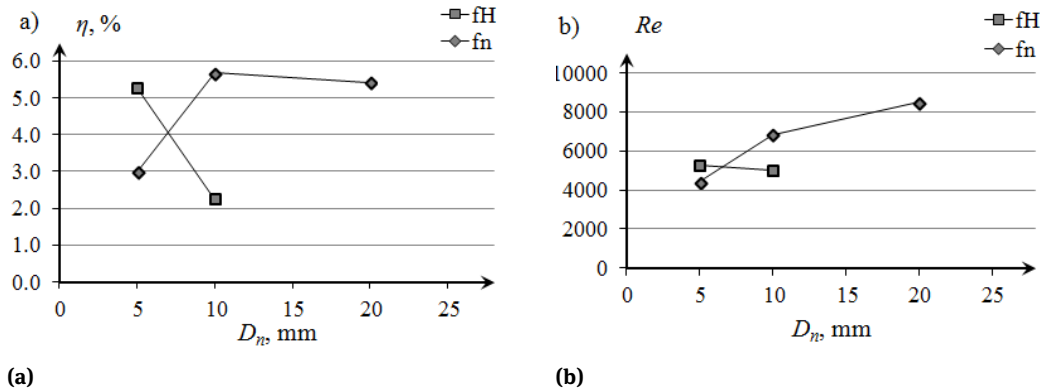


Figure 6: (a) actuator efficiency η and (b) Reynolds number Re as a function of nozzle diameter D_n for natural f_n and Helmholtz f_H resonance frequencies

The maximum efficiency $\eta = 8.67\%$ is obtained for f_n at $h = 15$ mm. The maximum $Re = 7900$ is obtained for f_n at $h = 15$ mm.

Figure 6 presents the dependence of actuator efficiency η and Reynolds number Re on the actuator cavity height for natural f_n and Helmholtz f_H frequencies.

The maximum efficiency $\eta = 5.67\%$ is obtained for f_n at $D_n = 10$ mm and it increases along with nozzle diameter change. Kordík and Trávníček [12] demonstrated that the dependence between nozzle diameter D_n and actuator efficiency η has the shape of a negative parabola. It is, therefore, necessary to accept that the optimal nozzle diameter D_n investigated actuators is in the range 5 to 20 mm – in case of natural frequency f_n . In the case of f_H , the biggest efficiency is at $D_n = 5$ mm. The maximum Reynolds number is obtained for f_n at $D_n = 20$ mm.

The dependence presented in Figure 5 and 6 are similar to the same dependence presented by Gil and Strzelczyk [13], although in this case, refer to acoustic SJA with two diaphragms rather than one.

6 Conclusion

Velocity measurements in a synthetic jet with two opposite diaphragms using a CTA have been presented in this paper. The measurements have been done using three different values of cavity height, nozzle diameter and for the frequency of power supply from $10 \div 1000$ Hz and one electric power 2 W. The SJA efficiency, Reynolds number and the stroke length have been presented for various configurations.

In the study, the theoretical and experimental values of natural and Helmholtz frequencies have been compared.

The error ranges from 27 to 60% and it depends on the used model and parameters of the actuators. The coupling ratio was calculated and it can also be used with an acoustic synthetic jet actuator with two diaphragms.

Efficiency and Reynolds number, as a function of the cavity height and the nozzle diameter, have been determined. Larger is the value of cavity height, the smaller is the value of efficiency and Reynolds number for natural frequency. The smaller is the value of nozzle diameter, the larger is the value of efficiency and Reynolds number for natural frequency. In the case of Helmholtz efficiency, these dependences are opposite. A similar relationship is observed for a synthetic jet actuator with one diaphragm.

Acknowledgement: This work was supported by the National Center for Research and Development, Poland. Grant No.: LIDER/6/0024/L-10/18/NCBR/2019.

References

- [1] Amitay, M., Honohan, A., Trautman, M. and Glezer, A.: Modification of the aerodynamic characteristics of bluff bodies using fluidic actuators, in *AIAA Paper 97-2004*, **1997**.
- [2] Ciuryla, M., Liu, Y., Farnsworth, J., Kwan, C. and Amitay, M.: Flight Control Using Synthetic Jets on a Cessna 182 Model, *J. Aircr.* **44**, 642–653, **2007**.
- [3] Krieg, M. and Mohseni, K.: Dynamic modeling and control of biologically inspired vortex ring thrusters for underwater robot locomotion, *IEEE Trans. Robot.* **26**, 542–554, **2010**.
- [4] Krieg, M. and Mohseni, K.: Modelling circulation, impulse and kinetic energy of starting jets with non-zero radial velocity, *J. Fluid Mech.* **719**, 488–526, **2013**.
- [5] Chaudhari, M., Puranik, B. and Agrawal, A.: Heat transfer characteristics of synthetic jet impingement cooling, *Int. J. Heat Mass Transfer* **53**, 1057–1069, **2010**.

- [6] Qayoum, A. and Malik, A.: Influence of the Excitation Frequency and Orifice Geometry on the Fluid Flow and Heat Transfer Characteristics of Synthetic Jet Actuators, *Fluid Dyn.* **54**, 575–589, **2019**.
- [7] Trávníček, Z., Tesar, V., Broučková, Z. and Peszynski, K.: Annular impinging jet controlled by radial synthetic jet, *Heat Transfer Eng.* **35**, 1450–1461, **2014**.
- [8] Tesař, V., Broučková, Z., Kordík, J., Trávníček, Z. and Peszynski, K.: Valves with flow control by synthetic jets, *EPJ Web Conf.* **25**, 01092, **2012**.
- [9] Gil, P.: Bluff body drag control using synthetic jet, *J. Appl. Fluid Mech.* **12**, 293–302, **2019**.
- [10] Kordík, J. and Trávníček, Z.: Comparison of synthetic jet actuators based on sharp-edged and round-edged nozzles, *EPJ Web Conf.* **143**, 02053, **2017**.
- [11] Kordík, J. and Trávníček, Z.: Maximization of integral outlet quantities of an axisymmetric synthetic jet actuator based on a loudspeaker, *EPJ Web of Conferences* **114**, 02152, **2016**.
- [12] Kordík, J. and Trávníček, Z.: Optimal diameter of nozzles of synthetic jet actuators based on electrodynamic transducers, *Exp. Therm. Fluid Sci.* **86**, 281–294, **2017**.
- [13] Gil, P. and Strzelczyk, P.: Performance and efficiency of loudspeaker driven synthetic jet actuator, *Exp. Therm. Fluid Sci.* **76**, 163–174, **2016**.
- [14] Greco, C.S., Ianiro, A., Astarita, T. and Cardone, G.: On the near field of single and twin circular synthetic air jets, *Int. J. Heat Fluid Flow* **44**, 41–52, **2013**.
- [15] Greco, C.S., Castrillo, G., Crispo, C.M., Astarita, T. and Cardone, G.: Investigation of impinging single and twin circular synthetic jets flow field, *Exp. Therm. Fluid Sci.* **74**, 354–367, **2016**.
- [16] Kordík, J., Trávníček, Z. and Pavelka, M.: Energetic efficiencies of synthetic and hybrid synthetic jet actuators driven by electrodynamic transducers, *Exp. Therm. Fluid Sci.* **69**, 119–126, **2015**.
- [17] Trisno, R., Harinaldi and Kosasih, E.A.: Vortex ring formation characteristics in synthetic jet due to changes of excitation frequency in the $1/2$ -ball cavity actuator, *J. Phys.: Conf. Ser.* **822**, 012010, **2017**.
- [18] Fanning, E., Persoons, T. and Murray, D.B.: Heat transfer and flow characteristics of a pair of adjacent impinging synthetic jets, *Int. J. Heat Fluid Flow* **54**, 153–166, **2015**.
- [19] Paolillo, G., Greco, C.S. and Cardone, G.: The evolution of quadruple synthetic jets, *Exp. Therm. Fluid Sci.* **89**, 259–275, **2017**.
- [20] Ahmad, M. and Qayoum, A.: Investigation of impingement of double orifice synthetic jet for heat and fluid flow characteristics in quiescent flow, *Pertanika J. Sci. Technol.* **27**, 1181–1206, **2019**.
- [21] Smyk, E.: Numerical simulation of axisymmetric valve operation for different outer cone angle, *EPJ Web Conf.* **143**, 02112, **2017**.
- [22] Pick, P. and Andrie, M.: The influence of modulated slotted synthetic jet on the bypass of Hump, *Eng. Mech.* **20**, 271–280, **2013**.
- [23] P. Pick, P., Skála, V. and Matějka, M.: Efficiency of active flow control by a synthetic jet around a Hump, *EPJ Web Conf.* **45**, 01075, **2013**.
- [24] Smyk, E.: Interference in axisymmetric synthetic jet actuator, *EPJ Web Conf.* **143**, 02111, **2017**.
- [25] Smyk, E.: Comparison of acoustic synthetic jet actuator with one and two diaphragms, in: *24th International Conference Engineering Mechanics 2018*, 777–780, **2018**.
- [26] Broučková, Z. and Trávníček, Z.: Visualization study of hybrid synthetic jets, *J. Visualization* **18**, 581–593, **2015**.
- [27] Smith, B.L. and Glezer, A.: Jet vectoring using synthetic jets, *J. Fluid Mech.* **458**, 1–34, **2002**.
- [28] Ahmad, M. and Qayoum, A.: Numerical Investigation of Dimensionless Numbers on Macro-scale Synthetic Jet Actuator in Quiescent Flow, *Tec. Ital. J. Eng. Sci.* **63**, 59–64, **2019**.
- [29] Gil, P.: Synthetic jet Reynolds number based on reaction force measurement, *J. Fluids Struct.* **81**, 466–478, **2018**.
- [30] Gil, P. and Smyk, E.: Synthetic jet actuator efficiency based on the reaction force measurement, *Sensors Actuators, A Phys.* **295**, 405–413, **2019**.
- [31] Trávníček, Z., Broučková, Z. and Kordík, J.: Formation criterion for axisymmetric synthetic jets at high stokes numbers, *AIAA J.* **50**, 2012–2017, **2012**.
- [32] Holman, R., Utturkar, Y., Mittal, R., Smith, B.L. and Cattafesta, L.: Formation criterion for synthetic jets, *AIAA J.* **43**, 2110–2116, **2005**.
- [33] Girfoglio, M., Greco, C.S., Chiatto, M. and de Luca, L.: Modelling of efficiency of synthetic jet actuators, *Sens. Actuators, A* **233**, 512–521, **2015**.
- [34] de Luca, L., Girfoglio, M. and Coppola, G.: Modeling and Experimental Validation of the Frequency Response of Synthetic Jet Actuators, *AIAA J.* **52**, 1733–1748, **2014**.